

Original Research Article

## Numerical Simulation of Straight Cylindrical Supersonic Exhaust Diffuser for High Altitude Rocket Engine

R. C. Mehta, G. Natarajan

Department of Aeronautical Engineering, Noorul Islam University, Kumaracoil 629180, Tamil Nadu, India

### \*Corresponding author

R. C. Mehta

Email: [drrakhab.mehta@gmail.com](mailto:drrakhab.mehta@gmail.com)

**Abstract:** A numerical analysis is carried out to determine the flowfield and starting characteristics of a straight cylindrical supersonic exhaust diffuser of a high-altitude simulation of a high expansion ratio rocket nozzle. The flow field inside the high-altitude facility is analyzed for a conical nozzle of expansion ratio of 25, diffuser inlet-to-nozzle throat area ratio of 28.9, and diffuser length-to-diameter ratio of 11.7. The variations of enthalpy with entropy are shown for the conical nozzle and the straight cylindrical supersonic exhaust diffuser in order to understand the thermodynamic behavior of the flow field. The evacuation performance of supersonic exhaust diffuser under steady operation and associated flow behaviors during the starting of the diffuser are analyzed with help of the Mach contour plots. The starting and break down conditions are achieved when at exit pressure of the nozzle is approximately equal to vacuum chamber pressure. The present numerically simulation delineates complex flowfield inside the diffuser very close to the starting condition.

**Keywords:** CFD, Rocket, Nozzle, Propulsion, Supersonic diffuser

### INTRODUCTION

The upper stage of a rocket engine of a satellite launch vehicle is customarily built with a high-expansion ratio rocket nozzle for generating maximum thrust at a low pressure environment. A high-altitude test (HAT) facility is required to evaluate the performance of the rocket motor under static conditions. The HAT facility with a low back pressure simulates the rocket nozzle of high altitude conditions. Supersonic exhaust diffusers (SED) are employed during ground-level tests of high altitude rocket motors to obtain low back pressures at the supersonic nozzle exit. Sufficient reduction in the back pressure inside the diffuser allows engine tests to be conducted without shock-induced flow separation occurring in the divergent section of the nozzle. A straight cylindrical SED with no secondary gas injection has been employed owing to its simplicity and a small outlay. A constant area SED has been considered an important device for the reduction of supersonic to subsonic velocity of the exhaust. The straight cylindrical SED can simulate low pressure environment for evaluating steady-state performance of a rocket nozzle. Immediately after the rocket motor is started, exhaust plume begins to expand from the nozzle exit and entrains the air inside the vacuum chamber due to the static pressure which is higher than the initial

chamber pressure and the momentum transfer by high speed nozzle exhaust flow. The chamber achieves its highest vacuum level and provides a low pressure environment in the vicinity of the nozzle exit while simulating high altitude conditions.

Goethert [1] has carried out experimental investigation using the straight cylindrical SED. Their experimental studies have revealed that the starting stagnation pressure for a diffuser is a function of the geometrical parameters and the operating conditions of the rocket motor. Annanamalai *et al.* [2] obtained experimentally a scaling factor for the SED. The challenging task in designing such a diffuser is to keep the facility length shorter and starting pressure ratio as low as possible. Massier and Roschke [3] have conducted experimental studies to find out the influence of SED configuration on pressure recovery. Park *et al.* [4] made a small-scale HAT facility to evaluate the flowfield of various types of SED. A lab-scale high-altitude simulator [5, 6] was set-up to analyze the complex flowfield of the SED performance in conjunction with the experimental and the numerical methods. Sivo, Meyer and Peters [7] describe the use of the various types of SED for the High Altitude Test facility. The challenging task in designing such a

diffuser is to keep the facility length shorter and starting pressure ratio as low as possible.

A schematic of axisymmetric straight cylindrical SED is depicted in Fig. 1. The straight cylindrical is attached with a vacuum chamber. The vacuum chamber isolates the rocket nozzle from the outside atmosphere and enables the measurement of full motor propulsive thrust by simulating the high-altitude environment. The gradual pressure recovery up to the atmospheric pressure is accomplished in the SED by means of a complex shock train system. An essential criterion to achieve the starting mode of the diffuser is that the flow at the entrance plane of the diffuser should be at supersonic velocity. As the chamber pressure is increased further, the straight cylindrical SED also flows full and the shock system is fully established in the duct. The over-all pressure ratio at the point where the nozzle-exit pressure just reaches its minimum value is termed as the starting pressure ratio.

The above literature survey reveals that the flow field features inside the conical convergent-divergent nozzle and the SED are complex and difficult to visualize experimentally. The satisfactory running of the SED needs a number of pressure measurements in order to evaluate its performance. The purpose of the present numerical analysis is to study steady flow analysis in the straight cylindrical SED. The starting behavior of the diffuser operation is required for better understanding of the complex flowfield features inside the SED. The Reynolds-averaged Navier-Stokes (RANS) equations are used with a low Reynolds number turbulence model [8] and are solved using FLUENT [9] flow solver. The variations of enthalpy with entropy will help to understand the complex flow inside the conical nozzle and the SED. Flowfield features of nozzle-unstarting/starting, and diffuser-unstarted/started mode are obtained for  $A_e/A^* = 25.0$ ,  $A_D/A^* = 28.9$  and  $L/D = 11.7$ . The numerical results are properly validated with the experimental data of Sivo *et al.* [7].

### Numerical Analysis

The axisymmetric time-dependent compressible turbulent Reynolds-Averaged Navier-Stokes equations considered in the present analysis are in strong conservation form and are solved using the FLUENT [9] software. The one-equation turbulence model proposed by Spalart-Allmaras [8] is employed to compute eddy viscosity.

The following initial and boundary conditions are applied in the numerical analysis for the compressible and viscous flow inside the SED as depicted in Fig. 1. At the solid wall, no-slip condition

is enforced together with adiabatic wall condition and the turbulent kinematic viscosity is set to zero at the wall. The over-all pressure ratio  $P_0/p_a$  of 19.9, 23.1, 29.0 and 43.3 are used for numerical simulations. Symmetry conditions are prescribed at the centerline of the straight cylindrical SED.

### Nozzle and SED Geometry

The axisymmetric conical nozzle has a convergent angle 30 deg and throat diameter  $D^* = 0.03$  m. The semi-cone angle of the divergent section of the nozzle is 15 deg. The nozzle exit diameter is  $D_e = 0.15$  m and is located at  $L = 0.185$  m from the throat. The area ratio of the exit-to-throat  $A_e/A^*$  is 25.0. The length and diameter of the diffuser is 1.887 m and 0.161 m, respectively.

### Computational Grid

The computational grid of SED is generated using Gambit version-2.1 [9], and the governing fluid dynamics equations are solved using FLUENT- 6.2, a finite volume based commercial CFD flow solve. A fully coupled implicit compressible flow solver with Spalart-Allmaras turbulence model [8] has been used to compute the flow pattern inside the diffuser system.

The numerical simulations of the above mentioned equations are carried out until the residues fall below  $1.0 \times 10^{-6}$  for all the flow variables. To investigate the sensitivity of the grid in the axial and radial directions, a numerical investigation is performed for various grid sizes of  $120 \times 60$ ,  $160 \times 60$ ,  $120 \times 80$ , and  $180 \times 50$ . The present numerical simulations were carried out on  $120 \times 80$ . The value of viscous sub-layer is kept above 26. Thus, the first computational grid is in the buffer layer of the turbulent boundary layer.

### RESULTS AND DISCUSSION

We initially analyze the flow field inside the conical nozzle using the Fluent. Figure 2 shows the density contour plots. It can be seen from the figure the mach disc, oblique shock striking to the nozzle wall and expanded flow. Figure 3 shows the variations of the centre line and wall pressure. The sudden pressure drop shows the presence of shock inside the nozzle. Figure 4 displays the enthalpy with entropy variation for the conical nozzle. All the flow field features can be noticed in the variations of the enthalpy with entropy. The nozzle throat is located at the point where the minimum enthalpy is occurred.

Now we simulate the flow field inside the SED. The experimental studies on HAT facility have been mainly to focus on examining the steady evacuation quality of the straight cylindrical SED as depicted in Fig. 1. The variation of the enthalpy vs

entropy is shown in Fig. 5. It reveals the complex thermodynamic behavior of the flow field inside the SED.

The Mach contour plots are depicted in Fig. 6 for different pressure ratio  $P_o/p_a$ . It displays the flowfield information and starting phenomenon of the SED. At low pressure ratio  $P_o/p_a$  ( $= 19.9$  and  $23.1$ ), the nozzle exhaust does not have enough momentum to drive the normal shock wave out of the nozzle. As a result, the flow separates in the nozzle divergent portion. But neither the nozzle nor the diffuser flows became full with the exhaust. As  $P_o/p_a$  increases from  $29.0$  to  $43.3$ , the exhaust flow fills the entire cross section of the nozzle, without any flow separation inside the nozzle. The oblique shock wave attached to the lip of the nozzle gives rise to a series of Mach discs that seal the vacuum-chamber from any back-flow that helps to maintain the low vacuum level in the chamber. It is important to note that the Mach discs are seen in the diffuser duct facilitate a gradual recovery of pressure. The shock system in the diffuser moves downstream as  $P_o/p_a$  increases. When the  $P_o/p_a$  is reduced below a minimum value of about  $23$ , the shock system moves into the nozzle and thus affected the expansion process in the nozzle. At  $P_o/p_a$  above  $23$ , supersonic flow is seen in the nozzle divergent section.

Thereafter, a compression shock system increases the pressure in the diffuser to approximately ambient pressure at the diffuser exit. The nozzle is underexpanded and the exhaust plume fully fills the diffuser.

The influence of  $p_e/P_o$  versus  $P_o/p_a$  on the starting characteristics of the SED is shown in Fig. 7. The shock structure developed in the diffuser blocks the vacuum chamber from any ingress of atmospheric air from the ambient. It is observed that the pressure level in the vacuum test decreases as the stagnation pressure increases up to a critical value ( $P_o/p_a \sim 23.1$ ), and beyond that, the test chamber pressure ratio  $p_e/P_o$  remains constant at about  $0.0025$ , irrespective of the  $P_o/p_a$ . The starting and the break down pressure ratio  $P_o/p_a$  is approximately about  $23$  as depicted in Fig. 7.

The wall static pressure variations measured [7] and calculated  $p_w/P_o$  with respect to  $x/D^*$  are shown in Fig. 8 for  $P_o/p_a$  of  $19.9$ ,  $23.1$ ,  $29.0$  and  $43.3$ . The experimental values are marked as symbols and numerical result represented by lines and the nozzle exit plane is also depicted in Fig. 8. The comparisons between the measured [7] and the computed wall pressure  $p_w/P_o$  are found to be in good agreement.

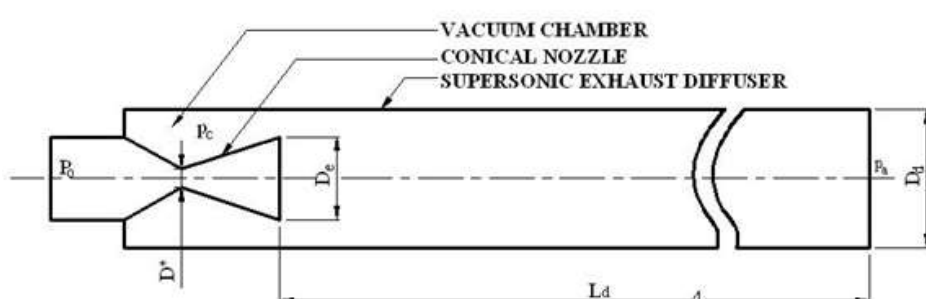


Fig. 1: Schematic of the SED geometry

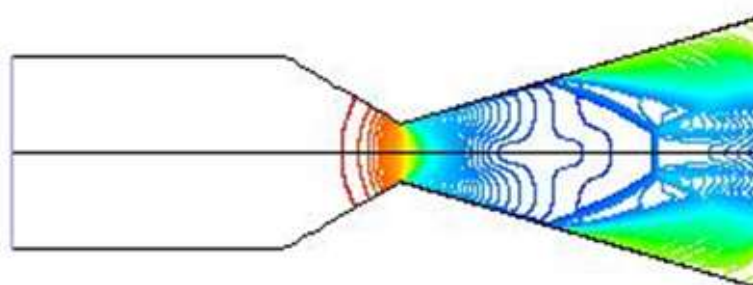
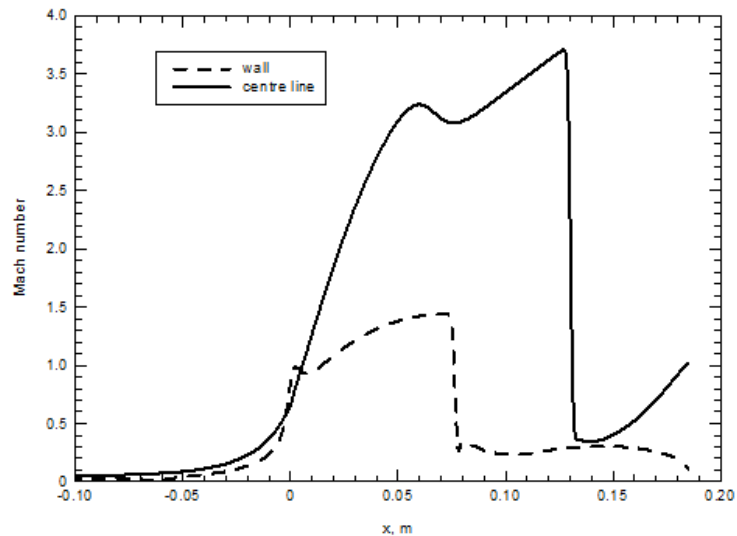
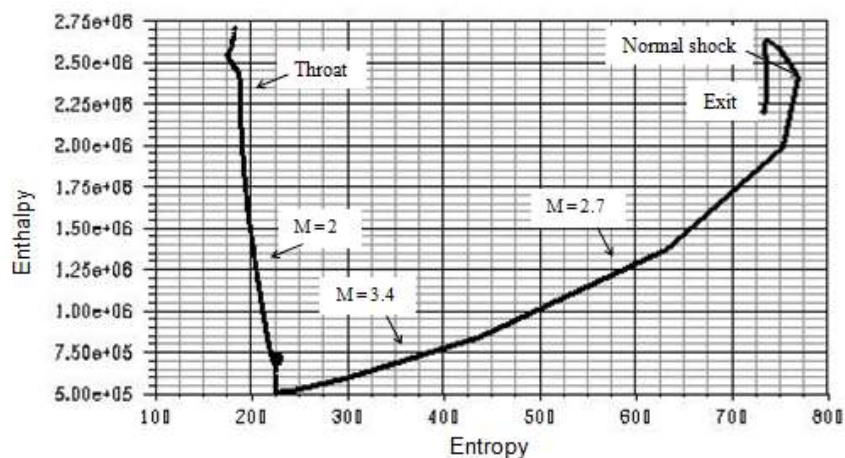


Fig. 2: Density contours for the conical nozzle



**Fig- 3:Variation of pressure inside the conical nozzle**



**Fig-4: Variation of enthalpy vs. entropy inside the conical nozzle**

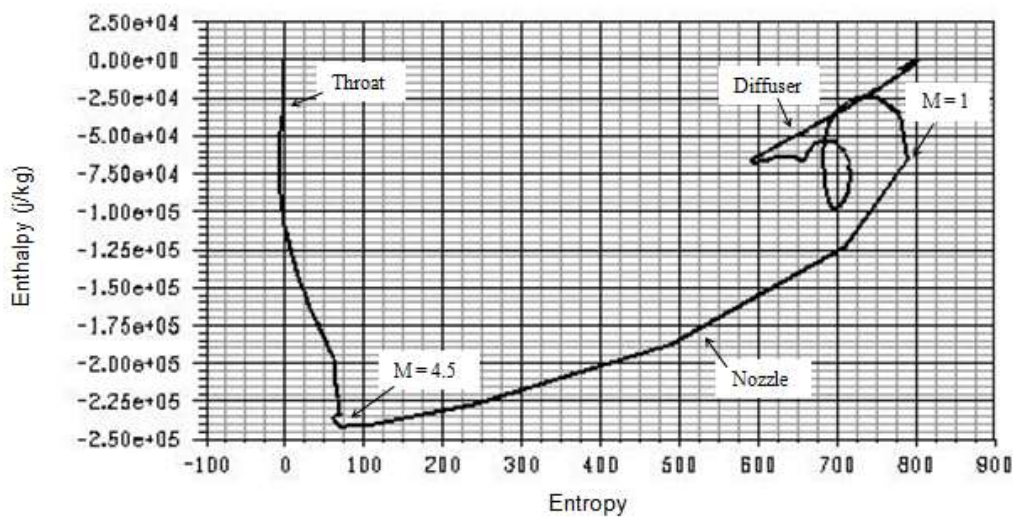


**Fig-5:Variation of enthalpy vs. entropy inside the SED**

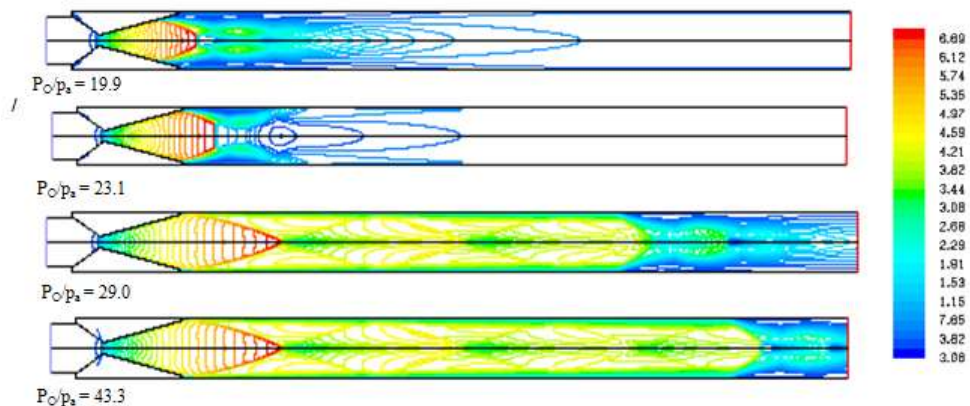


**Fig. 6** Mach contour plots for various value of  $P_o/p_a$

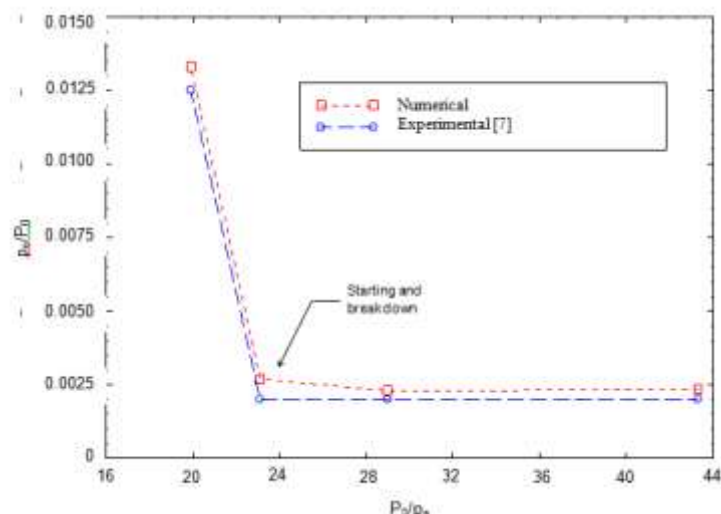


**Fig. 7** Wall static pressure variations for various value of  $P_o/p_a$

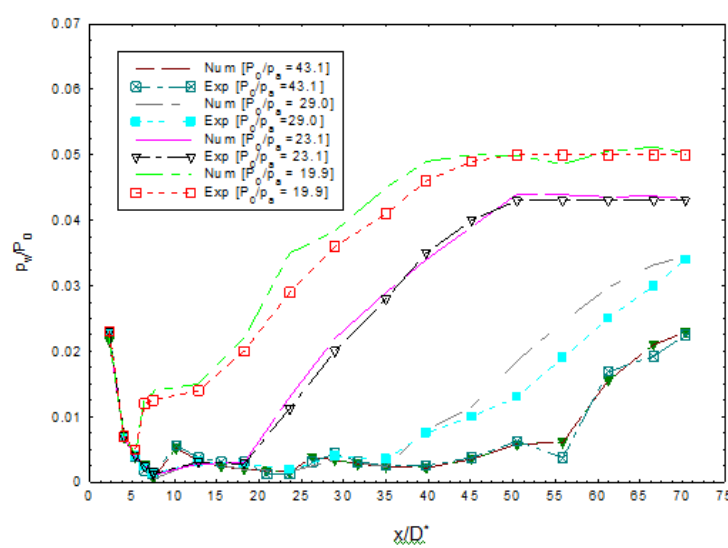


**Fig.8:** Variation of  $p_e/P_o$  versus  $P_o/p_a$

### Nomenclature

$A$ =	Area, m <sup>2</sup>
$D$ =	diameter of diffuser, m
$L$ =	length of diffuser, m
$M$ =	Mach number
$P$ =	total pressure, Pa
$p$ =	static pressure, Pa
$t$ =	time, s
Subscripts	
$a$ =	ambient
$c$ =	vacuum
$D$ =	diffuser
$e$ =	exit of nozzle
$o$ =	stagnation
$w$ =	wall
Superscript	
$*$ =	throat

### CONCLUSIONS

A numerical simulation of the straight cylindrical SED is performed to find out the minimum  $P_o/p_a$  to establish and maintain full expansion of the nozzle flow. The straight cylindrical SED is having  $A_e/A^*$  of 25,  $A_D/A^*$  of 28.9 and  $L/D$  of 11.7. The starting behavior of the straight cylindrical SED is analyzed using computational fluid dynamics approach. The RANS equations solved using FLUENT software with one-equation turbulence model. A complex flowfield is observed inside the straight cylindrical SED by the present numerical simulation. The variations of enthalpy vs. entropy reveal the thermodynamic behavior of inside the conical nozzle and the SED. The starting condition of the diffuser flows is investigated in conjunction with experiment results [7]. The measured wall pressure of Sivo *et al.* [7] along the diffuser shows good agreement with the numerical results. The numerical simulation has captured the fully filled flow in the SED with the train of the shock wave.

### REFERENCES

1. Goethert BH; High altitude and space simulation testing, ARS Journal, 1962; 32(6): 872-882.
2. Annamalai K, Vishnathan K, Sriramulu V, Bhskaran KA; Evaluation of the performance of supersonic exhaust diffuser using scaled down models, *Experimental Thermal and Fluid Science*, 1998; 17: 217-229
3. Massier PF, Roschke EJ; Experimental investigation of exhaust diffusers for rocket engines, *Progress in Astronautics and Rocketry: Liquid Rockets and Propellants*, Vol. 2, Academic Press, NY, 1960; 3-75.
4. Park BH, Lee JH, Yoon W; Studies on the starting transient of a straight cylindrical supersonic exhaust diffuser: Effects of diffuser length and pre-evacuation state, *International Journal of Heat and Fluid Flow*, 2008; 29: 1369-1379.
5. Yeom HW, Yoon S, Sung HG; Flow dynamics at the minimum starting condition of a supersonic diffuser to simulate a rocket's high altitude performance on the ground, *Journal of Mechanical Science and Technology*, 2009; 23: 256-263.
6. Sung HG, Yeom HW, Yoon S, Kim SJ, Kim J; Investigation of rocket exhaust diffusers for altitude simulation, *Journal of Propulsion and Power*, 2010; 26(2): 240-247.
7. Sivo JN, Meyer CL, Peters DJ; Experimental Evaluation of Rocket Exhaust Diffusers for Altitude Simulation, NASA TN D-298, 1960.
8. Spalart P, Allmaras S; A One-Equation Turbulence Model for Aerodynamic Flows, AIAA paper 92-0439, 1992.
9. Fluent 6.2, Computational Fluid Dynamics Software User Guide, Fluent Inc., Fluent India Pvt Ltd., 2010.